Establishing a Au Nanoparticle Size Effect in the Oxidation of Cyclohexene Using Gradually Changing Au Catalysts

Baira G. Donoeva,[†,‡,§] Daniil S. Ovoshchnikov,[†,§] and Vladimir B. Golovko*[,†,‡]

[†]Department of Chemistry, University of Canterbury, 20 Kirkwood Avenue, Christchurch 8041, New Zealand
[‡]The MacDiarmid Institute for Advanced Materials and Nanotechnology, Wellington 6140, New Zealand

S *Supporting Information*

ABSTRACT: The effect of the size of gold nanoparticles on their catalytic activity in aerobic oxidation of cyclohexene was established using supported gold nanoparticles that gradually undergo a change in size during the catalytic reaction. Two triphenylphosphine-stabilized clusters, $Au_9(PPh_3)_8(NO_3)_3$ and $Au_{101}(PPh_3)_{21}Cl_5$, were synthesized and deposited on SiO_2. The clusters did not retain their structure during the catalytic reaction; larger particles with mean diameters of ~5−10 nm gradually formed. By combining kinetic experiments with the monitoring of catalyst transformations using transmission electron microscopy, diffuse-reflectance ultraviolet−visible spectroscopy, and X-ray photoelectron spectroscopy, we showed that catalytic activity appeared only after >2 nm Au^0 particles had formed, while intact clusters and phosphine-free <2 nm particles were inactive in cyclohexene oxidation under the studied conditions.

KEYWORDS: gold nanoparticles, gold clusters, oxidation, catalysis, size effect
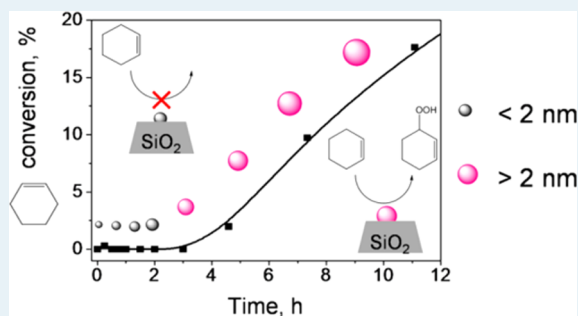
■ INTRODUCTION

Gold had long been considered chemically inactive, until Haruta and Hutchings discovered remarkable catalytic properties of gold nanoparticles in their pioneering works.[1,2] Since that discovery, gold nanoparticles have been shown to be active in various reactions, including low-temperature CO oxidation, C−C bond formation, selective hydrogenation and oxidation, etc.[3−5] One of the crucial parameters determining the catalytic activity of gold is the size of gold particles; e.g., only <5 nm particles are active in the low-temperature CO oxidation, and their activity increases with a decrease in particle size.[6−9] Attempts were also made to establish particle size effects for the liquid-phase oxidation reactions catalyzed by supported gold nanoparticles. However, opposite trends in the effects of Au particle size on their catalytic activity in the same reactions are frequently reported.[10−16] Typically, particle size effects are studied by comparing catalytic activities within a series of supported gold nanoparticles with different mean diameters that are assumed to be constant during the reaction.[12,14,17,18] Gold particles within such series are often prepared using different wet chemistry methods, which could affect the catalytic activity, thus obscuring the effect of particle size. Such an influence could be eliminated by employing gold particles that gradually undergo a change in size during the catalytic reaction. Because catalytic activity can be observed only when active sites are present, simultaneous monitoring of the catalytic activity and the state of catalyst in such a gradually changing system could provide insight into the optimal catalyst morphology. In this work, we employed silica-supported phosphine-stabilized Au clusters with initial sizes of <2 nm

and studied their activity in the aerobic oxidation of cyclohexene used as a model reaction. We found that the clusters were unstable during the reaction and gradually agglomerated to form larger particles. By combining the investigation of cyclohexene oxidation kinetics with the monitoring of catalyst transformations, we established a size effect of Au nanoparticles on their catalytic activity.

■ RESULTS AND DISCUSSION

The triphenylphosphine-stabilized gold cluster, $Au_9(PPh_3)_8(NO_3)_3$ (Au_9), and gold nanoparticles with an estimated composition of $Au_{101}(PPh_3)_{21}Cl_5$ (Au_{101}), with mean gold core diameters of 0.9 and 1.5 nm, respectively, were immobilized on SiO_2. The catalysts were denoted by xAu_n/SiO_2, where x indicates the Au loading (weight percent). The catalysts were tested in the aerobic solvent-free oxidation of cyclohexene at 65 °C. Four major products formed during the reaction: cyclohexene oxide, 2-cyclohexen-1-ol, 2-cyclohexen-1-one, and cyclohexenyl hydroperoxide (the latter being the main product). We observed an induction period in the oxidation of cyclohexene, catalyzed by as-made Au_n/SiO_2. The length of the induction period depended on the Au loading of the catalyst (Figure 1A). The decrease in the Au loading of Au_9/SiO_2 from 0.5 to 0.02 wt % led to the elongation of the induction period from ~1 to ~6.5 h. The length of the induction period also depended on the type of Au cluster: $0.1Au_{101}/SiO_2$ showed a
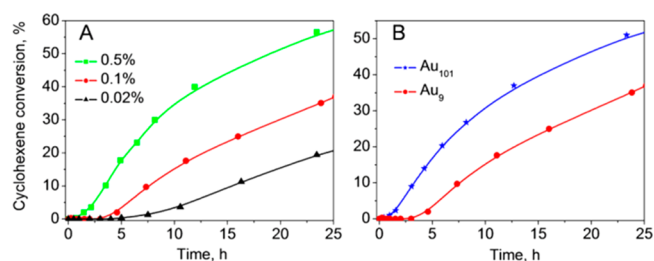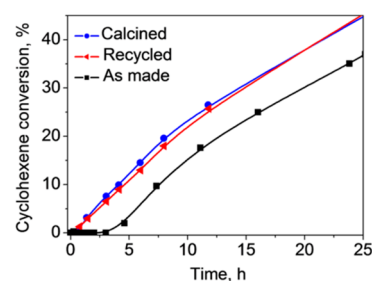
Figure 1. Cyclohexene oxidation catalyzed by (A) Au$_9$/SiO$_2$ with gold loadings of 0.5, 0.1, and 0.02 wt % and (B) 0.1Au$_{101}$/SiO$_2$ and 0.1Au$_9$/SiO$_2$. Conditions: solvent-free cyclohexene, 10 mL, 1 atm of O$_2$, 65 °C, 0.1 g of catalyst.

significantly shorter induction period of 50 min compared with 3.5 h for 0.1Au$_9$/SiO$_2$ (Figure 1B).

The change in the Au particle size during the reaction was monitored using transmission electron microscopy (TEM) and diffuse-reflectance UV−visible spectroscopy (DR UV−vis). TEM micrographs of 0.5Au$_9$/SiO$_2$ sampled from the reaction after 0.5, 1, and 16 h are shown in panels B−D of Figure 2, respectively. Intact Au$_9$ clusters of as-made 0.5Au$_9$/SiO$_2$ are not visible on bright-field TEM images because of the poor contrast for the supported <1 nm Au clusters (Figure 2A). During the reaction, larger particles, which can be detected by TEM, gradually form, and their number increases, as evidenced by the increase in the surface density of visible particles. Approximately 40, 170, and 370 particles/μm^2 were detected in TEM micrographs of 0.5Au$_9$/SiO$_2$ sampled from the reaction after 0.5, 1, and 16 h, respectively. The mean diameter of detectable particles was 3.1 ± 1.2 nm after 1 h and increased further to 5.4 ± 1.4 nm over the next 15 h. The development of the particle size as a function of reaction time for 0.5Au$_9$/SiO$_2$ is shown in Figure S7 of the Supporting Information.

The DR UV−vis study of 0.5Au$_9$/SiO$_2$ showed the appearance of the surface plasmon resonance (SPR) band at 520 nm for samples of catalyst recovered from the reaction after 1 h. The appearance of the SPR band indicates the formation of >2 nm gold particles (Figure 2E).[19−21] Hence, both TEM and

DR UV−vis studies of 0.5Au$_9$/SiO$_2$ show similar times of formation of >2 nm particles. DR UV−vis studies of 0.1Au$_9$/SiO$_2$ and 0.02Au$_9$/SiO$_2$ showed that >2 nm particles form only after ~4 and ~6.5 h, respectively. Slower gold agglomeration for catalysts with lower Au loadings is most likely due to the lower density of Au particles on the SiO$_2$ surface. As seen from the kinetics of cyclohexene oxidation (Figure 1A) and DR UV−vis data, in all cases the formation of a sufficient number of >2 nm particles was accompanied by the appearance of catalytic activity, which indicates that such particles are active in cyclohexene oxidation. The absence of an induction period for Au$_9$/SiO$_2$, recycled after a 16 h catalytic run, supports this conclusion (Figure 3).

Figure 3. Cyclohexene oxidation catalyzed by as-made, recycled, and precalcined 0.1Au$_9$/SiO$_2$.

Importantly, the cyclohexene used for catalytic oxidation did not contain 2,6-di-*tert*-butyl-4-methylphenol, which is typically added as a stabilizer by chemical suppliers. When we used cyclohexene that contained the stabilizer, the Au$_9$ clusters did not agglomerate after 16 h under typical reaction conditions (65 °C and 1 atm of O$_2$) and no cyclohexene conversion was observed. Stirring 0.5Au$_9$/SiO$_2$ for 16 h under typical reaction conditions, but in *n*-hexane instead of cyclohexene, also did not lead to cluster agglomeration. These results imply that thermal treatment at 65 °C alone is not enough to induce agglomeration of Au$_9$ supported on SiO$_2$. Recently, Kilmartin et al. reported the removal of phosphine ligands from silica-
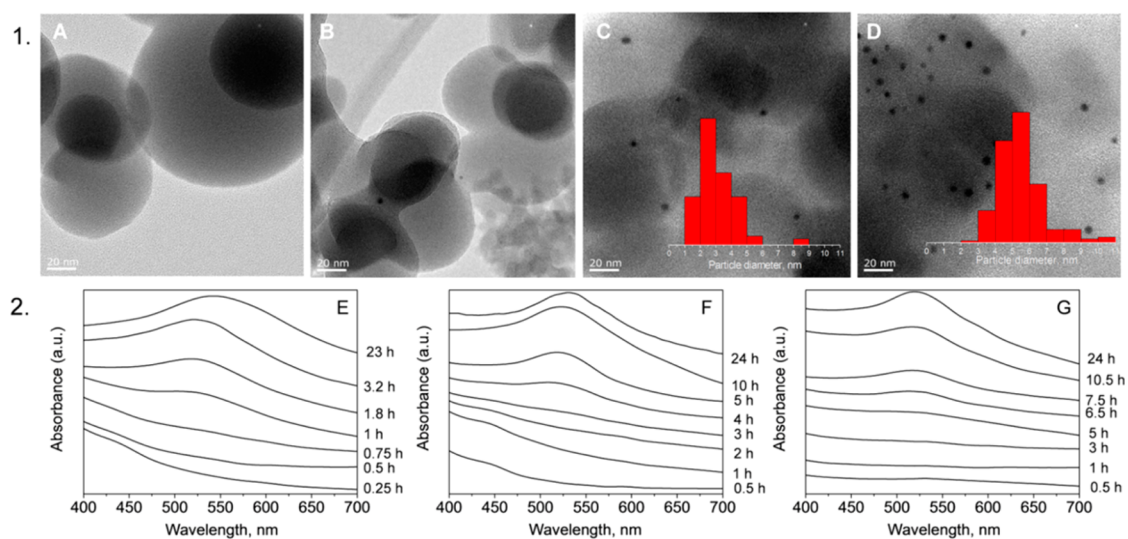
Figure 2. (A−D) TEM micrographs of as-made 0.5Au$_9$/SiO$_2$ (A) and 0.5Au$_9$/SiO$_2$ sampled from the reaction after 0.5 (B), 1 (C), and 16 h (D). (E−G) DR UV−vis spectra of 0.5Au$_9$/SiO$_2$ (E), 0.1Au$_9$/SiO$_2$ (F), and 0.02Au$_9$/SiO$_2$ (G) sampled at reaction times indicated along the right-hand ordinates.

supported Au$_6$[Ph$_2$P(o-tolyl)]$_6$(NO$_3$)$_2$ by $tert$-butyl hydroperoxide.[22] We suggest that in our case phosphine ligands were removed from the cluster via reaction with cyclohexenyl hydroperoxide (CyOOH), which is present in trace amounts in the stabilizer-free cyclohexene [~0.015 wt % by gas chromatography (GC)]. Agglomeration did not occur in n-hexane or stabilized cyclohexene because neither of them contained even traces of peroxides. Thus, cluster agglomeration is possible only when PPh$_3$ ligands are removed from the gold core of Au$_9$. An indication of such step-by-step in $situ$ transformation of gold clusters, which includes the removal of the ligands from the cluster cores and subsequent particle agglomeration, can also be seen in Figure 2F. DR UV−vis spectra of the catalyst sampled in the initial stages of the reaction possessed a weak band at 450 nm, originating from intact Au$_9$ clusters (Figure S1C of the Supporting Information). The features in the optical spectra of small phosphine-stabilized gold clusters are known to be due to the effects of the ligand shell bound to the gold core of the cluster.[23] Therefore, the disappearance of the band at 450 nm before the SPR band emerges indicates that agglomeration occurs after the ligand shell is at least partially removed. Because sintering is not possible when ligands are still bound to the gold cores of the clusters, we conclude that particles forming during the reaction are predominantly phosphine-free.

Pure Au$_9$ clusters lose phosphine ligands upon calcination at 230 °C for 40 min in an Ar flow according to TGA (Figure S3 of the Supporting Information). Calcination of 0.1Au$_9$/SiO$_2$ under the same conditions to remove phosphine ligands from supported Au$_9$ led to the formation of 8.0 ± 2.6 nm particles (Figure S10 of the Supporting Information). A catalyst treated this way showed a cyclohexene conversion profile similar to that of the recycled 0.1Au$_9$/SiO$_2$ [particle size of 9.6 ± 3.9 nm (Figure S8B of the Supporting Information)], which indicates that phosphine-free particles similar in size and larger than 2 nm obtained in different ways have similar activity in the reaction (Figure 3).

Inasmuch as two catalyst parameters change during the reaction, i.e., Au particle size and the presence of phosphine ligands, the initial inactivity of the as-made catalysts could be due to one of the following. (a) Stabilizing ligands cover active gold sites, thus hindering catalytic activity; once the phosphine ligands are removed, the particles become active. (b) The <2 nm gold particles, even without phosphine ligands, are inactive in cyclohexene oxidation, and activity appears only after the particle size reaches a certain threshold. Results of our experiments indicate that removal of phosphine ligands is not a sufficient condition for the appearance of catalytic activity and particle size plays a significant role. (a) As seen from Figure 2F, the PPh$_3$ ligand shell was at least partially removed from Au$_9$ after 2 h, as indicated by disappearance of the band at 450 nm, but no activity was observed until >2 nm particles had formed after ~4 h (Figure 1A). (b) Because the core of Au$_{101}$ is larger than that of Au$_9$, gold particles derived from Au$_{101}$ need significantly less time to overcome the threshold in particle size, which leads to a shorter induction period for the Au$_{101}$ catalyst (Figure 1B).

To confirm that small (<2 nm) and phosphine-free Au particles are inactive in cyclohexene oxidation, we deposited Au$_9$ on SBA-15,[24] a mesoporous SiO$_2$-based material with a large surface area (see the Supporting Information for details). We used a mixture of ethanol and dichloromethane to ensure a homogeneous distribution of clusters throughout the surface of

the support.[25] To remove phosphine ligands from the cluster core, the catalyst was calcined at 230 °C for 40 min in an Ar flow (denoted as 0.1Au$_9$/SBA_c230). The large surface area of the support and the homogeneous distribution of clusters prevented particles from sintering during calcination, as evidenced by the absence of the SPR band in the DR UV−vis spectrum of 0.1Au$_9$/SBA_c230 (Figure 4). On the other
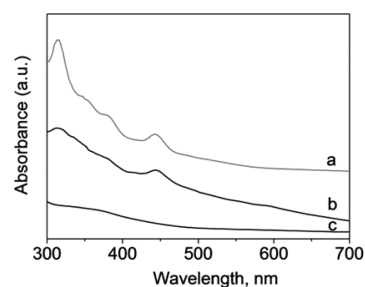
Figure 4. UV−vis spectrum of Au$_9$ dissolved in CH$_2$Cl$_2$ (a) and DR UV−vis spectra of as-made 0.1Au$_9$/SBA-15 (b) and 0.1Au$_9$/SBA_c230 (c).

hand, the absence of absorption bands at 450, 380, and 315 nm, characteristic of the Au$_9$ cluster, indicates successful removal of ligands during calcination. TEM of 0.1Au$_9$/SBA_c230 also confirmed very minimal agglomeration; only a few 2−3 nm particles were detected, which correlates with the results obtained for Au$_{11}$ clusters in a similar system.[25] Thus, phosphine-free <2 nm particles supported on SBA-15 were obtained.

Although the Au particles were phosphine-free, the kinetics of cyclohexene oxidation in the presence of 0.1Au$_9$/SBA_c230 showed an induction period of ~3.5 h. The appearance of catalytic activity correlated with the formation of plasmonic particles (Figure 5), which was similar to the behavior observed
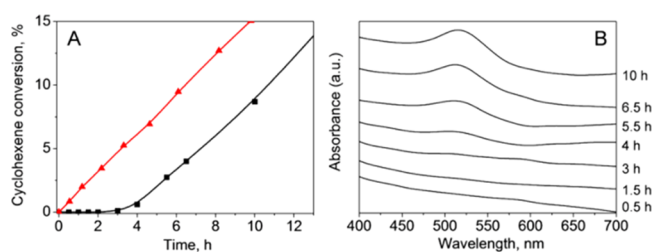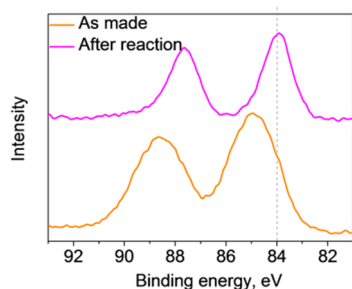

Figure 5. (A) Cyclohexene oxidation catalyzed by 0.1Au$_9$/SBA_c230 (black) and recycled 0.1Au$_9$/SBA_c230 (red). (B) DR UV−vis spectra of 0.1Au$_9$/SBA_c230 sampled from cyclohexene oxidation at different reaction times.

for SiO$_2$-based catalysts, discussed earlier. Recycled 0.1Au$_9$/SBA_c230 did not show an induction period in cyclohexene oxidation. This result confirmed that phosphine-free <2 nm Au particles are inactive in cyclohexene oxidation. The change in the catalytic behavior of Au particles once they become larger than 2 nm could be due to the transition from nonmetallic to metallic properties, which occurs at sizes of ~2 nm.[26]

Numerous examples of catalysis, driven or enhanced by the surface plasmon resonance of Au nanoparticles, have been recently reported.[27−29] Because catalytic activity in our study appeared only when >2 nm gold nanoparticles, i.e., plasmonic particles, were formed, we investigated whether the observed activity was enabled by the SPR. The activity of 0.5Au$_9$/SiO$_2$ in

cyclohexene oxidation under ambient light was similar to that in the absence of light, which indicated that catalytic activity was not enhanced by the SPR in this study (Table S2 of the Supporting Information).

The X-ray photoelectron spectroscopy (XPS) spectrum of a postreaction $0.5Au_9/SiO_2$ showed the Au $4f_{7/2}$ signal centered at 84.0 eV, a binding energy characteristic of bulk neutral gold (Figure 6). No signal at 85.0 eV from pristine Au_9 clusters[30]

Figure 6. XPS Au $4f_{7/2}$ spectra of as-made $0.5Au_9/SiO_2$ and $0.5Au_9/SiO_2$ recovered after a 16 h catalytic cycle of cyclohexene oxidation. The dotted vertical line indicates the Au $4f_{7/2}$ peak position corresponding to metallic gold.

was detected in the postreaction catalyst, indicating that most of the gold present in the catalytic system is in the metallic state and no intact clusters are left after the reaction. Unlike the recently reported activity of positively charged 20−150 nm Au nanoparticles in styrene oxidation,[11] catalytic activity in our case was solely due to the metallic Au^0 particles, as evidenced by the activity of the postreaction catalysts in the second catalytic cycle.

Finally, colloid stabilizer-free[31] and citrate-stabilized[32] Au nanoparticles were synthesized and deposited onto SiO_2 with a total gold loading of 0.1 wt %. Four catalysts ($0.1Au-9.1/SiO_2$, $0.1Au-13.7/SiO_2$, $0.1Au-33.9/SiO_2$, and $0.1Au-47.4/SiO_2$ with particle sizes of 9.1, 13.7, 33.9, and 47.4 nm, respectively) were obtained (Figure S11 of the Supporting Information). All the catalysts were active in cyclohexene oxidation, and no induction period was observed (Figure 7). Comparison of initial reaction
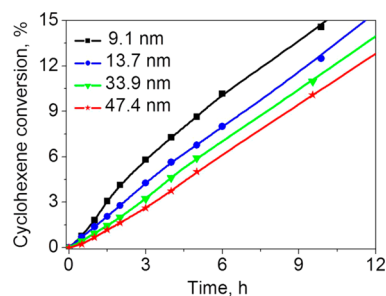
Figure 7. Cyclohexene oxidation catalyzed by 9.1, 13.7, 33.9, and 47.4 nm Au particles supported on SiO_2 with a total gold loading of 0.1 wt %.

rates and turnover frequencies (TOFs) of the Au colloid-based catalysts is shown in Table 1. The catalytic activity of $0.1Au/SiO_2$ gradually decreased with an increase in Au particle size, which is in accordance with the smaller fraction of surface Au atoms for larger particles. Indeed, TOF values normalized by surface Au are very close for differently sized supported Au nanoparticles (Table 1). This result confirms that >2 nm Au^0

particles are responsible for the observed catalytic activity in the oxidation of cyclohexene.

In this work, we showed that only >2 nm Au^0 particles were active in aerobic cyclohexene oxidation; however, oxygen adsorption and its dissociative activation on large metallic gold particles were shown to be extremely impeded.[33,34] On the other hand, extended gold surfaces were long known to catalyze the abstraction of hydrogen from hydrocarbons,[35] and thus, activation of cyclohexene rather than O_2 by gold nanoparticles is the more probable pathway in our case. This suggestion is also supported by the fact that the main product of cyclohexene oxidation in this work is cyclohexenyl hydroperoxide (Figure S12 of the Supporting Information), which is formed in the reaction between dissolved oxygen and cyclohexenyl radicals generated via abstraction of allylic hydrogen from cyclohexene. When a sufficient amount of cyclohexenyl hydroperoxide is formed, it further acts as a radical chain propagator in cyclohexene autoxidation.[36] A similar mechanism was recently described for cyclohexane oxidation catalyzed by Au/MgO.[37] The higher activity of Au catalysts in cyclohexene oxidation compared to that in cyclohexane oxidation[12,37,38] can be explained by more facile abstraction of hydrogen from an allylic position because the allylic C−H bond is weaker than the alkylic C−H bond.

Thus, we showed that at low temperatures <2 nm particles are not able to catalyze the abstraction of hydrogen from the cyclohexene and >2 nm metallic Au particles are the active sites associated with the observed catalytic activity. Such a size effect is the opposite of that discovered for oxidation reactions in which O_2 activation is involved, e.g., styrene oxidation, for which either <2 nm particles[10,34] or large, positively charged particles[11] were suggested as the active sites.

In summary, we established a relationship between the size of supported gold nanoparticles and their activity in solvent-free aerobic oxidation of cyclohexene by employing gradually changing catalysts. We showed that phosphine-stabilized gold clusters and <2 nm phosphine-free Au particles are inactive in this reaction, and that catalytic activity appears only upon formation of a sufficient number of >2 nm metallic particles. A further increase in Au particle size results in a gradual decrease in catalytic activity, which correlates with a decrease in Au surface area. The size dependency observed in this study is in agreement with the suggested mechanism of substrate activation through the abstraction of hydrogen catalyzed by metallic gold nanoparticles.

■ EXPERIMENTAL SECTION

Materials. Gold (99.99%), sodium borohydride (>97%), hydrochloric acid (37%, AR grade), dichloromethane (99.8%), ethanol (99.99%), *n*-decane (99%), *n*-hexane (98%), nitric acid (65%, AR grade), triphenylphosphine (98%), Pluronic P123 ($M_n \sim 5800$), tetraethyl orthosilicate (98%), cyclohexene (99%, inhibitor-free), 2-cyclohexen-1-ol (95%), 2-cyclohexen-1-one (98%), and cyclohexene oxide (98%) were purchased from Sigma-Aldrich and Merck. Oxygen (99.7%) was obtained from BOC gases. Silicon oxide (Aerosil OX 50) was purchased from Evonik. All materials were used as received.

Catalyst Preparation. $Au_9(PPh_3)_8(NO_3)_3$ (Au_9) and $Au_{101}(PPh_3)_{21}Cl_5$ (Au_{101}) were synthesized according to the published procedures.[39,40] As-made gold clusters were deposited onto SiO_2 from a CH_2Cl_2 solution. A calculated amount of gold cluster dissolved in CH_2Cl_2 (10 mL, 1−2 mg/mL) was added dropwise to a vigorously stirred suspension of

Table 1. Comparison of Initial Reaction Rates and TOFs of Au/SiO₂ Catalysts in Cyclohexene Oxidation

	catalyst	reaction rate ($\times 10^6$ mol of substrate/s)	TOF_{Au} (s^{-1})	$TOF_{surface\ Au}$ (s^{-1})
1	$0.1Au\text{-}9.1/SiO_2$	0.58	1.14	17.5[a]
2	$0.1Au\text{-}13.7/SiO_2$	0.39	0.78	18.0[a]
3	$0.1Au\text{-}33.9/SiO_2$	0.28	0.53	21.7[b]
4	$0.1Au\text{-}47.4/SiO_2$	0.20	0.40	18.9[b]

[a]Fraction of surface Au atoms estimated assuming a spherical shape of Au nanoparticles (based on TEM observations). [b]Fraction of surface Au atoms estimated assuming a cuboctahedral shape of Au nanoparticles (based on TEM observations).

SiO_2 (500 mg) in CH_2Cl_2 (15 mL). The mixture was stirred for 30 min, and the solid was collected by centrifugation. A colorless supernatant solution confirmed complete cluster deposition. The catalysts were washed with CH_2Cl_2 (20 mL) and dried under vacuum at room temperature. Deposition of the Au_9 cluster onto SBA-15 was performed using a methodology similar to that described by Liu et al.[41] SBA-15 (500 mg) was suspended in the mixture of C_2H_5OH and CH_2Cl_2 (5 mL, 1:4). A solution of the Au_9 cluster (2.3 mg) in the same solvent mixture (5 mL) was slowly added to the suspension of SBA-15 while it was being vigorously stirred. The mixture was stirred for 2.5 h. The solid was collected via centrifugation, washed with CH_2Cl_2 (10 mL), and dried under vacuum at room temperature.

Stabilizer-free gold nanoparticles were synthesized using the method reported by Martin et al.[31] After deposition onto SiO_2, the average diameter of Au particles was 9.1 nm. Citrate-stabilized Au nanoparticles were prepared following a protocol described by Turkevich et al.[32] Briefly, 450 mL of a 0.24 mM $HAuCl_4$ and 1.6 mM sodium citrate solution was heated at 70 °C for 1 h. The resulting red solution containing 13.9 nm Au particles was cooled using an ice bath; 33.9 nm particles were prepared by heating 50 mL of a 0.3 mM $HAuCl_4$ and 0.58 mM sodium citrate solution at 90 °C for 5 min, and 47.4 nm particles were prepared by heating 50 mL of a 1.2 mM $HAuCl_4$ and 1.9 mM sodium citrate solution at 60 °C for 2 h. The resulting colloid Au particles were deposited on SiO_2 from aqueous solutions. A calculated volume of a fresh Au nanoparticle solution in water was added to SiO_2 (0.5 g). The mixture was sonicated for 1 min, and water was slowly removed from the suspension using a rotary evaporator. The resulting solid was collected, dried under vacuum at room temperature, and characterized using TEM.

Catalyst Characterization. Catalysts were characterized using TEM, XPS, and DR UV–vis. Gold loadings were established using atomic absorption spectroscopy (AAS) on a Varian SpectrAA 220FS instrument. TEM analysis was performed using a Philips CM200 instrument operating at 200 kV. Samples for TEM analysis were suspended in diethyl ether and deposited on holey carbon-coated Cu grids. At least 100 particles were measured to plot size distributions. DR UV–vis spectra were recorded using a Cintra 404 (GBC Scientific Equipment) spectrometer. XPS was conducted on a Kratos Axis DLD spectrometer with a monochromated Al Kα X-ray source. The samples were pressed into indium as the mounting medium. A supply of low-energy electrons was used for charge neutralization. Survey spectra were recorded with a pass energy of 80 eV and high-resolution spectra with a pass energy of 40 eV. Binding energies were normalized with respect to the position of the adventitious C1s peak at 285.0 eV.

Catalytic Experiments. The catalytic activity of Au catalysts was tested in aerobic solvent-free cyclohexene oxidation without addition of a radical initiator. Kinetic studies of cyclohexene oxidation were performed in a glass reactor equipped with a reflux condenser. Ten milliliters of cyclohexene containing 0.2 M *n*-decane as an internal standard, 100 mg of catalyst, and a Teflon-coated magnetic stirrer were loaded into a 100 mL two-neck glass round-bottom flask. The system was flushed with O_2 three times and connected to a rubber balloon filled with O_2. The mixture was magnetically stirred at 65 °C. Samples of the reaction mixture were taken using a glass syringe. The reaction was stopped by cooling the reactor to room temperature; the condenser was rinsed with 5 mL of diethyl ether, and the reaction mixture was separated from the solid catalyst by centrifugation. Catalysts were washed with diethyl ether and dried under vacuum at room temperature before being recycled. Each experiment was reproduced at least three times. The typical standard errors of independent catalytic tests were <1.5%. Turnover frequencies were calculated from the initial rates of cyclohexene oxidation.

The liquid samples were analyzed by gas chromatography (GC-FID) using a Shimadzu GC-2010 instrument equipped with an Rxi-5SilMS capillary column (30 m × 0.25 mm × 0.25 μm). The products of cyclohexene oxidation were identified by GC–mass spectrometry (Shimadzu GCMS-QP2010) and quantified using solutions of reference compounds at known concentrations. The concentration of cyclohexenyl hydroperoxide was established using iodometric titration.[42] Addition of PPh₃ to the reaction mixture prior to GC analysis did not change the concentration of 2-cyclohexen-1-one, determined from GC analysis, which implies that there was no decomposition of cyclohexenyl hydroperoxide during GC analysis.[43] The concentration of cyclohexenyl hydroperoxide was calibrated by comparison of GC data and iodometric titration results and was further calculated directly from GC results.

■ ASSOCIATED CONTENT

Ⓢ Supporting Information

Cluster and catalyst characterization details and additional catalytic data. This material is available free of charge via the Internet at http://pubs.acs.org.

■ AUTHOR INFORMATION

Corresponding Author

*E-mail: vladimir.golovko@canterbury.ac.nz.

Author Contributions

§B.G.D. and D.S.O. contributed equally to this work.

Notes

The authors declare no competing financial interests.

■ ACKNOWLEDGMENTS

■ REFERENCES

(1) Haruta, M.; Kobayashi, T.; Sano, H.; Yamada, N. *Chem. Lett.* **1987**, 405.

(2) Hutchings, G. J. *J. Catal.* **1985**, *96*, 292.

(3) Corma, A.; Garcia, H. *Chem. Soc. Rev.* **2008**, *37*, 2096.

(4) Stratakis, M.; Garcia, H. *Chem. Rev.* **2012**, *112*, 4469.

(5) Della, P. C.; Falletta, E.; Rossi, M. *Chem. Soc. Rev.* **2012**, *41*, 350.

(6) Haruta, M. *Catal. Today* **1997**, *36*, 153.

(7) Haruta, M. *J. New Mater. Electrochem. Syst.* **2004**, *7*, 163.

(8) Hvolbæk, B.; Janssens, T. V. W.; Clausen, B. S.; Falsig, H.; Christensen, C. H.; Nørskov, J. K. *Nano Today* **2007**, *2*, 14.

(9) Schubert, M. M.; Hackenberg, S.; van Veen, A. C.; Muhler, M.; Plzak, V.; Behm, R. J. *J. Catal.* **2001**, *197*, 113.

(10) Turner, M.; Golovko, V. B.; Vaughan, O. P. H.; Abdulkin, P.; Berenguer-Murcia, A.; Tikhov, M. S.; Johnson, B. F. G.; Lambert, R. M. *Nature* **2008**, *454*, 981.

(11) Wang, L.; Zhang, B.; Zhang, W.; Zhang, J.; Gao, X.; Meng, X.; Su, D. S.; Xiao, F.-S. *Chem. Commun.* **2013**, *49*, 3449.

(12) Liu, Y.; Tsunoyama, H.; Akita, T.; Xie, S.; Tsukuda, T. *ACS Catal.* **2011**, *1*, 2.

(13) Xu, L.-X.; He, C.-H.; Zhu, M.-Q.; Wu, K.-J.; Lai, Y.-L. *Catal. Lett.* **2007**, *118*, 248.

(14) Haider, P.; Kimmerle, B.; Krumeich, F.; Kleist, W.; Grunwaldt, J.-D.; Baiker, A. *Catal. Lett.* **2008**, *125*, 169.

(15) Haider, P.; Urakawa, A.; Schmidt, E.; Baiker, A. *J. Mol. Catal. A: Chem.* **2009**, *305*, 161.

(16) Liu, Y.; Tsunoyama, H.; Akita, T.; Tsukuda, T. *Chem. Lett.* **2010**, *39*, 159.

(17) Sun, K.-Q.; Luo, S.-W.; Xu, N.; Xu, B.-Q. *Catal. Lett.* **2008**, *124*, 238.

(18) Tana; Wang, F.; Li, H.; Shen, W. *Catal. Today* **2011**, *175*, 541.

(19) Kamat, P. V. *J. Phys. Chem. B* **2002**, *106*, 7729.

(20) Kelly, K. L.; Coronado, E.; Zhao, L. L.; Schatz, G. C. *J. Phys. Chem. B* **2003**, *107*, 668.

(21) Henglein, A. *Langmuir* **1999**, *15*, 6738.

(22) Kilmartin, J.; Sarip, R.; Grau-Crespo, R.; Di, T. D.; Hogarth, G.; Prestipino, C.; Sankar, G. *ACS Catal.* **2012**, *2*, 957.

(23) Woehrle, G. H.; Hutchison, J. E. *Inorg. Chem.* **2005**, *44*, 6149.

(24) Zhao, D.; Feng, J.; Huo, Q.; Melosh, N.; Frederickson, G. H.; Chmelka, B. F.; Stucky, G. D. *Science* **1998**, *279*, 548.

(25) Liu, Y.; Tsunoyama, H.; Akita, T.; Tsukuda, T. *J. Phys. Chem. C* **2009**, *113*, 13457.

(26) Bond, G. C.; Thompson, D. T. *Catal. Rev.* **1999**, *41*, 319.

(27) Vankayala, R.; Sagadevan, A.; Vijayaraghavan, P.; Kuo, C.-L.; Hwang, K. C. *Angew. Chem., Int. Ed.* **2011**, *50*, 10640.

(28) Sun, M.; Xu, H. *Small* **2012**, *8*, 2777.

(29) Christopher, P.; Xin, H.; Linic, S. *Nat. Chem.* **2011**, *3*, 467.

(30) Battistoni, C.; Mattogno, G.; Cariati, F.; Naldini, L.; Sgamellotti, A. *Inorg. Chim. Acta* **1977**, *24*, 207.

(31) Martin, M. N.; Basham, J. I.; Chando, P.; Eah, S.-K. *Langmuir* **2010**, *26*, 7410.

(32) Turkevich, J.; Stevenson, P. C.; Hillier, J. *Discuss. Faraday Soc.* **1951**, *11*, 55.

(33) Janssens, T. V. W.; Clausen, B. S.; Hvolbaek, B.; Falsig, H.; Christensen, C. H.; Bligaard, T.; Norskov, J. K. *Top. Catal.* **2007**, *44*, 15.

(34) Alves, L.; Ballesteros, B.; Boronat, M.; Cabrero-Antonino, J. R.; Concepción, P.; Corma, A.; Correa-Duarte, M. A.; Mendoza, E. *J. Am. Chem. Soc.* **2011**, *133*, 10251.

(35) Bond, G. C. *Gold Bull. (Geneva)* **1972**, *5*, 11.

(36) Mahajani, S. M.; Sharma, M. M.; Sridhar, T. *Chem. Eng. Sci.* **1999**, *54*, 3967.

(37) Conte, M.; Liu, X.; Murphy, D. M.; Whiston, K.; Hutchings, G. J. *Phys. Chem. Chem. Phys.* **2012**, *14*, 16279.

(38) Lue, G.; Ji, D.; Qian, G.; Qi, Y.; Wang, X.; Suo, J. *Appl. Catal., A* **2005**, *280*, 175.

(39) Weare, W. W.; Reed, S. M.; Warner, M. G.; Hutchison, J. E. *J. Am. Chem. Soc.* **2000**, *122*, 12890.

(40) Wen, F.; Englert, U.; Gutrath, B.; Simon, U. *Eur. J. Inorg. Chem.* **2008**, *2008*, 106.

(41) Liu, Y.; Tsunoyama, H.; Akita, T.; Tsukuda, T. *J. Phys. Chem. C* **2009**, *113*, 13457.

(42) Mair, R. D.; Graupner, A. J. *Anal. Chem.* **1964**, *36*, 194.

(43) Shul'pin, G. B. *J. Mol. Catal. A: Chem.* **2002**, *189*, 39.